Effect of different thickness of material filter on Tc-99m spectra and performance parameters of gamma camera

A Nazifah[1], S Norhanna[1], S I Shah[1] and A Zakaria[2]

[1] International Islamic University Malaysia, Kuantan, 25200, Pahang, Malaysia
[2] University Sains Malaysia, Kubang Kerian, 16150, Kelantan, Malaysia

E-mail: nazifah@unisza.edu.my

Abstract: This study aimed to investigate the effects of material filter technique on Tc-99m spectra and performance parameters of Philip ADAC forte dual head gamma camera. Thickness of material filter was selected on the basis of percentage attenuation of various gamma ray energies by different thicknesses of zinc material. A cylindrical source tank of NEMA single photon emission computed tomography (SPECT) Triple Line Source Phantom filled with water and Tc-99m radionuclide injected was used for spectra, uniformity and sensitivity measurements. Vinyl plastic tube was used as a line source for spatial resolution. Images for uniformity were reconstructed by filtered back projection method. Butterworth filter of order 5 and cut off frequency 0.35 cycles/cm was selected. Chang's attenuation correction method was applied by selecting 0.13/cm linear attenuation coefficient. Count rate was decreased with material filter from the compton region of Tc-99m energy spectrum, also from the photopeak region. Spatial resolution was improved. However, uniformity of tomographic image was equivocal, and system volume sensitivity was reduced by material filter. Material filter improved system's spatial resolution. Therefore, the technique may be used for phantom studies to improve the image quality.

1. Introduction

Nuclear medicine imaging is considered as an important modality amongst the other medical imaging techniques. It can provide physiological information at the molecular and cellular level that leads to the determination of health conditions. It can be categorized into, planar and tomography. Tomography is most commonly performed because it can provide the 3D information about physiologic functions of organ e.g, perfusion, and metabolism [1] and high diagnostic accuracy [2,3] which depends on the ability of the imaging device to detect differences in the uptake of a radiopharmaceutical in a lesion and its surroundings. The quality and details of images obtained by gamma cameras are affected by several parameters, such as spatial resolution, sensitivity and uniformity [4]. Further, NaI (Tl) detector of the gamma camera is unable to discriminate all scattered gamma photons due to poor energy resolution. That causes poor quality image and inaccuracy in the quantification of radiopharmaceutical uptake [5–7]. Thus scatter correction is important for absolute quantification of single photon emission computed tomography (SPECT) data reported [8–10]. As stated by Hutton [11] there are many scatter correction techniques developed in last 3 decades, but they have some drawbacks for routine implementation. Another technique which reduces some fraction of scatter by using a material filter applied in planar imaging by Pillay [12] which is an alloy filter consisting of Pb, Zn and Sn for patient studies and they discovered improvement in image

contrast and suggested this method may be used in SPECT. Study conducted by Pollard [13] for imaging therapeutic doses of -131, attaching physical filter of lead sheets (1.6mm - 6.4mm). In PET scanning, lead filters were used in order to reduce the number of scattered events [14]. Further, the effects of material filters, i.e., copper and aluminum to reduce scattered gamma photons in SPECT using phantom were studied by Shah [15]. Based upon the above findings, Zn material of different thicknesses was used as a material filter to investigate the effects on imge quality in SPECT.

2. Materials and methods

2.1. Calculation for selection of material filter.

Using equation 1 calculations were carried out for zinc (0.1 - 1 mm thicknesses) to determine the attenuation fraction of different gamma photon energies.

$$I = I_0 e^{-\mu x} \quad (1)$$

Where I_o is the intensity of the gamma photon beam before attenuation by the material, I is the intensity of the transmission gamma photons after passing through the material and μ is the linear attenuation coefficient (cm^{-1}) of material at a given energy of gamma photon, x is the thickness of the material. Linear attenuation coefficient (μ) values were taken from [16] for gamma photon energies ranging from 80 – 200 keV.

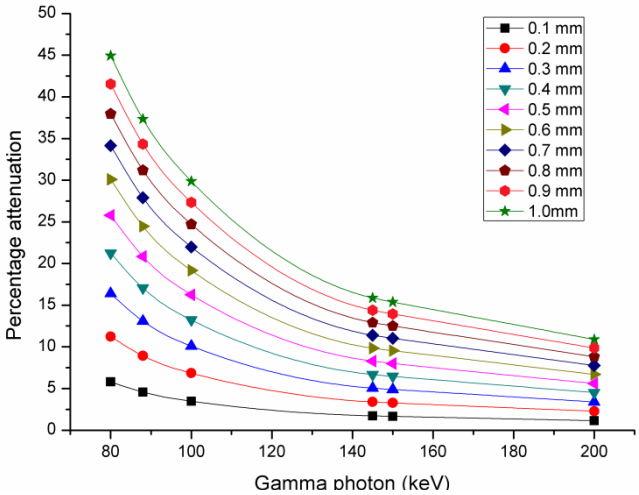

Figure 1. Percentage attenuation of gamma photon energies by various thickness of zinc.

Based on theoretical values, i.e., percentage difference of gamma photon energies attenuated by various thicknesses of material versus energy has been plotted as shown in Figure 1. As expected, the percentage of gamma photon attenuation decreases with increasing energy and increases with increasing thickness of material. However, the relative percentage attenuation of zinc 0.1 mm thick material is higher within the range of (92-139 keV) compared to 140 keV photons. But, due to the nonavailibility of 0.1 mm thickness, material filters of 0.198 mm and 0.4 mm thickness have been designed.

2.2. Planar data acquisition

2.2.1. Measurement of energy spectra of Tc 99m. Cylindrical source tank of NEMA SPECT Triple Line Source Phantom (20.2 cm inner diameter and inner height 20 cm) was filled with water and Tc-99m (15 mCi) was injected. Mineral water was used to make sure that there are no dust particles. After that, small amount of ink was added to provide a visual indication of the distribution of the activity. Cylindrical phantom was shaken gently for uniform distribution of radioactivity. Cylindrical tank was placed on the patient couch closer to the low energy high resolution *(LEHR)* collimator face in the central FOV of a gamma camera *(Philip ADAC Forte dual head)*. Matrix size was used is 64 x 64 x 16. The energy window ranges, 54 – 160, 62-160, 70-160 keV until 156 – 160 keV. Duration of count rate measurement for every window without and with material filter was maintained at 5 seconds.

Scanning time and count rate for every reading in each energy window were recorded. Three readings for each window were recorded and corrected for decay.

2.2.2. Spatial resolution. To investigate the effect on spatial resolution of a material filter, a vinyl plastic tube having an inner diameter 0.8 mm and length 10 cm filled with a Tc-99m (1.36 mCi) was used as a line source. The acrylic plates (30 cm x 30 cm) of different thicknesses were employed as a uniform scattering medium (tissue equivalent) [17]. Data acquisition matrix size 64 x 64 x 16 was selected. 20% energy window centered at 140 keV was adjusted. Pixel size in the X-direction was calculated by dividing field of view (FOV) gamma camera 508 mm with number of pixels (64). The system spatial resolution was evaluated at a distance from 1 cm up to 10 cm in 1 cm increments collimator to source distance in air Figure 2 (a). Also with and without material filter figure 2 (b). Experimental setting was same as in the case of air but with an increment of scattering material thickness. Care was taken to make sure the position of line source to remain same every time while adding the scattering material. The time per image was maintained at 5 seconds. Line spread function (LSF) for every source to collimator distance was obtained from the line profiles. The gamma camera stores counts from a line source in a single view and count profile bell-shaped (Graph of counts per pixel vs distance along counts profile in pixels) was drawn perpendicularly to the line source at the same place for each data set. The count profiles of LSF was used to determine the full width at half maximum (FWHM) and full width at tenth (FWTM).

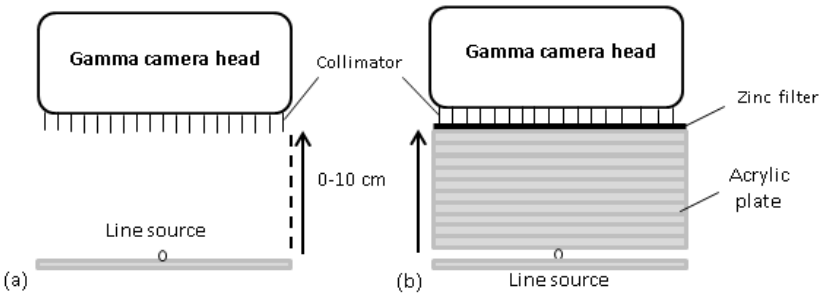

Figure 2. Arrangement for measurement of spatial resolution (a) without material filters (b) with scattering medium.

2.3. Tomography (SPECT) data acquisition

2.3.1. Uniformity. For tomographic uniformity data without and with material filter (0.198 mm and 0.4 mm) a cylindrical source tank of NEMA SPECT Triple Line Source Phantom with volume (6,409.48 cm^3), containing a homogeneous solution of Tc-99m (7.15 mCi) was used. Data collection parameters were chosen, such as; matrix size 128 x 128 x 16, clockwise rotation 360^0. Ninenty projections, 21 seconds per projection with 15 million total counts as recommended by [18], rotation radius of gamma camera head was fixed at 16.9 cm parallel to the axis of rotation. Energy window was 20% centered at 140 keV. SPECT images from the phantom data were reconstructed by filtered backprojection method. Butterworth filter of order 5, cut off frequency 0.35 cycles/cm was selected. Chang's attenuattion correction was applied by selecting 0.13/cm linear attenuation coefficient.

2.3.2. System volume sensitivity. Homogeneous solution of Tc 99m (16.74 mCi), 128 projections with 100, 000 counts per projection followed the same procedure as by [19]. The rest of the data collection parameters were used same as described in section 2.2.1.1. Activity and time to start and finish was recorded as shown in Table 1. System volume sensitivity was calculated using equation (17-15) and also volume sensitivity per axial, by dividing with diameter of cylindrical source tank [17].

Table 1. Activity, total scans time and total number of counts.

	Activity at scanning time (mCi)	Total time of scanning (hours)	Number of counts
Without filter	14.72	1.12	86, 682.08
Material 0.198 mm	13.97	1.55	82, 419.23
Material 0.4 mm	13.26	2.10	78, 063.93

3. Results and Discussion

3.1. Tc- 99m energy spectra.

Figure 2 shows that energy spectra of Tc 99m without and with material filter (0.198 mm and 0.4 mm) that was plotted by imaging cylindrical tank. As some scatter is present into photopeak region. This results maybe explained by the fact that gamma rays that have undergone large-angle scatters in the cylindrical tank and emerge with lower energy. This is significant problem that is encountered in clinical studies because scattered photons emit from the patient. With material filter, it should be noted that not only count rate in compton region is decreased but also in the photopeak region. That means it were reduce scatter portion in photopeak region. And this is seen clearly at compton and photopeak regions from the table 2. Research conducted by Kojima [20] show that in 125-139 keV region 75-80% are present and also stated by Hutton [11] about 30-40% scatter counts are in photopeak region. Results shows that when material filter 0.4 mm was applied it reduces more than double of counts as compared to material filter 0.198 mm for both of regions. So the most ideal filter here might be material filter 0.198 mm because reduces less count rate at 140 keV.

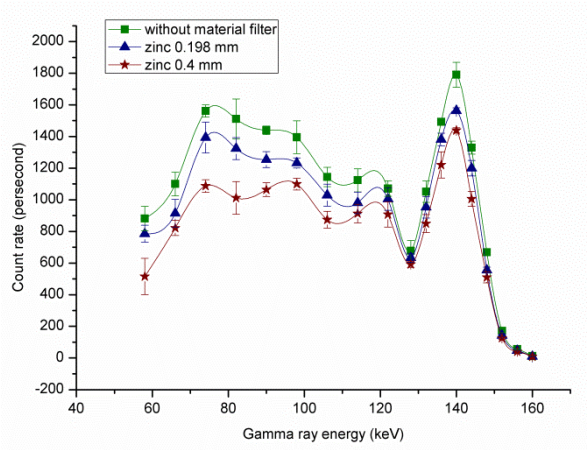

Figure 3. Energy spectra of Tc-99m without and with material filter (0.19 mm and 0.4 mm).

Table 2. Percentage reduction in count rate with material filter (0.198 mm and 0.4 mm).

Material thickness(mm)	Compton region	Photopeak region		
	92-125 keV	126-139keV	140 keV	141-154 keV
0.198	10.99%	8.75%	13.14%	12.87%
0.4	22.44%	18.49%	21.28%	26.45%

3.2. Spatial Resolution

From the Figure 4 and 5 the presence of scattering material degrade spatial resolution as compared to air. In this study, when material filter 0.198 mm was applied improvement in FWHM and FWTM below 7 and 5 cm source to collimator distance was obtained, respectively. Another finding was that FWHM and FWTM were degraded when material filter 0.4 mm was applied as compared to 0.198 mm. This is because of the increased thickness of material filter which has most probaly absorbed more unscattered events and also generated more scattered gamma photons. This finding is in agreement with ALehyani [21] statement that with the increase in source to collimator distance spatial resolution of the gamma camera was degraded.

3.3. Uniformity

Degree of uniformity over each transverse image of cylindrical phantom was evaluated by drawing count profile curves along the X-axis through the centre. Transverse image number twenty three was selected because it was more uniform as compared to other images. From the Figure 5 below we can see the count profile curve along the X- axis of the cylindrical phantom. However, no difference was observed in the count profile with both thicknesses of material filter (0.198 mm and 0.4 mm) as compared to without material filter. For the future research it is suggested for increase in the amount of Tc-99m.

3.4. System volume sensitivity

Table 3 shows that when a material filter 0.198 mm was applied, 5.69% reduction as compared to without material filter and that reduction increased to 13% when material filter 0.4 mm. Furthermore, results are similar to volume sensitivity per axial. These results might be due to absorption count through a material filter that have reduction in system volume sensitivity and also for volume sensitivity per axial.

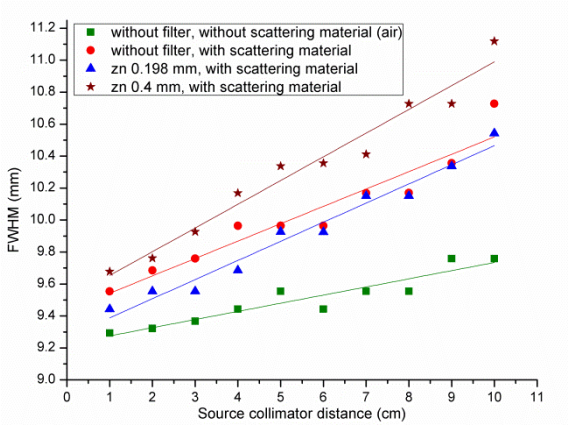

Figure 4. FWHM in air and in scattering medium (without and with material filter).

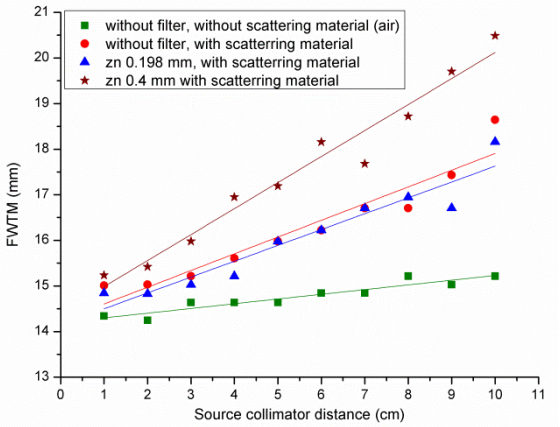

Figure 5. FWTM in air and in scattering medium (without and with material filter).

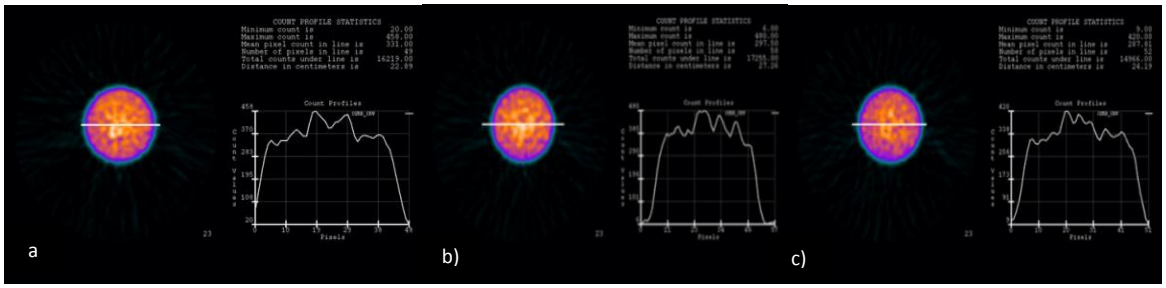

Figure 6. a) without and with material filter b) 0.198 mm and c) 0.4 mm.

Table 3. Concentration of radionuclide, total time acquisition, number of counts, system volume sensitivity and volume sensitivity per axial.

(mm)	A Concentration of radionuclide (Bq/mL)	T Time required to complete acquisition (sec)	N number of counts recorded	SVS (cps/Bg/mL)	Volume sensitivity per axial
Without material filter	84,974.13	1260	13215302	0.123	6.09×10^{-3}
Material 0.198	80,817.79	1320	12333928	0.116	5.74×10^{-3}
Material 0.4	76,545.99	1380	11279588	0.107	5.30×10^{-3}

4.Conclusion

With the use of material filter, it shows the count rate is decreased from compton and photopeak region of Tc-99m spectrum. Material filter 0.198 mm thickness improved spatial resolution, however, uniformity of tomographic images is equivocal, and system volume sensitivity has shown reduction as compared to without material filter. Therefore, based on spatial resolution results the material filter may be applied for improvement in image quality in Tc-99m planar and tomography. This technique reduce the scattered gamma photons from the raw data before image reconstruction. In terms of clinical implementation, it is easy and cost effective.

Acknowledgment

Authors are grateful to the Department of Nuclear Medicine, Oncology and Radiotheraphy Hospital Universiti Sains Malaysia, Kubang Kerian, Kelantan for the use of Gamma Camera and other facilities

to carry out this research work. Also thanks to School of Health Sciences Universiti Sains Malaysia for other support.

References

[1] Schaefer W M, Nowak B, Kaiser H, Koch K, Block S, Dahl J 2003 Comparison of Microsphere-Equivalent Blood Flow (^{15}O-Water PET) and Realtive Perfusion (^{99m}Tc-Tetrofosmin SPECT) in Myocardium Showing Metabolism – Perfusion Mismatch *J Nuc Med* **44** 33–9

[2] uz Zaman M 2007 99mTc-EC-deoxyglucose-- poor man's 18F-FDG: what will be the future of PET in molecular imaging? *Eur J Nucl Med Mol Imaging* **34** 429 doi:10.1007/s00259-006-02998-8

[3] Tamahi N, Tadamura E, Kudoh T 1997 Recent advances in nuclear cardiology in the study of coronary artery disease *Ann Nucl Med* **11** 55–66

[4] Lyra M, Ploussi A 2011 Filtering in SPECT Image Reconstruction *Int J Biomed Imaging* 1-14 doi: 10.1155/2011/693795

[5] Chuanyong B, Babla H, Conwell R 2010 Emission-Based Scatter Correction in SPECT Imaging *Tsinghua Sci Tehnol* **15** 1–10

[6] Hesse B, Tägil K, Cuocolo A, Anagnostopoulos C, Bardiés M, Bax J, et al 2005 EANM/ESC procedural guidelines for myocardial perfusion imaging in nuclear cardiology *Eur J Nucl Med Mol Imaging* **32** 855–97 doi: 10.1007/s00259-005-1779-y

[7] de Vries D J, King M A, Soares E J, Tsui B M W, Metz C E 1999 Effects of Scatter Subtraction on Detection and Quantitation in Hepatic SPECT *J Nucl Med* **40** 1011–1023

[8] Xiao J, de Wit T C, Staelens S G, Beekman F J 2006 Evaluation of 3D Monte Carlo – Based Scatter Correction for 99m Tc Cardiac Perfusion SPECT *J Nucl Med* **47** 1662–1669

[9] Celler A, IEEE M, Axent D, Toganet D, El-Khatib J 2000 Investigation of Scatter in SPECT Transmission Studies *IEEE Trans Nucl Sci* **47** 1251–1257

[10] Ljungberg M, King M A, Hademenos G J, Strand S 1993 Comparison of Four Scatter Correction Methods Using Monte Carlo Simulated Source Distributions *J Nucl Med* **35** 143–151

[11] Hutton B F, Buvat I, Beekman J F 2011 Review and current status of SPECT scatter correction *Phys Med Biol* **56** R85–R112 doi: 10.1088/0031-9155/56/14/R01

[12] Pillay M, Shapiro B, Cox P H 1986 The effect of an alloy filter on gamma camera images. Eur *J Nucl Med* **12** 293–5

[13] Pollard K R, Bice A N, Eary J F, Durack L D, Lewellen T K 1992. A Method for Imaging Therapeutic Doses of Iodine- 13 1 with a Clinical Gamma Camera *J Nucl Med* **33** 771–6

[14] Spinks T J, Shah S I 1993 Effect of lead filters on the performance of a Neuro-PET Tomography operated without septa *IEEE Trans Nucl Sci* **40** 1087–1091

[15] Shah S I, Zakaria A, Yee F S 2004 Effect of Unconventional Filters on Uniformty, Sensitivity and Linearity of an Imaging System in SPECT *Australas Phys Eng Sc* 27

[16] Hubbell J H, Seltzer S M 1996 NIST: X-Ray Mass Attenuation Coefficients Radiat Biomol Phys Div PML, NIST [cited 2014 Apr 14]; Available from: http://www.nist.gov/pml/data/xraycoef/

[17] International Commission on Radiation Units and Measurements (ICRU) [cited 2014 April Available from: http://www.icru.org/home/reports/tissue-substitutes-in-radiation-dosimetry-and-measurement-report-44

[18] Assurance Q, Systems S. IAEA Human Health Series No.6 Quality Assurance for SPECT Systems 6

[19] Cherry S R, Sorenson J A, Mutsumasa T, Phelps M E 2012 Physics in Nuclear Medicine. *Fourth edi. Elsevier Saunders*

[20] Kojima A, Matsumoto M, Mutsumasa T, Takahashi M 1991 Eksperimental analysis of scattered photons in Tc-99m imaging with a gamma camera *Ann Nucl Med* **5** 139–44

[21] ALehyani S H A 2009 Application of single photon emission computed tomography (SPECT) parameters for bone scintigraphy *J King Saud Univ* **21** 107-117